Electrostatic interaction between two nonuniformly charged colloid particles confined in a long charged cylinder wall

2008 J. Phys.: Condens. Matter 20 035109

(http://iopscience.iop.org/0953-8984/20/3/035109)

IOP PUBLISHING JOURNAL OF PHYSICS: CONDENSED MATTER

J. Phys.: Condens. Matter **20** (2008) 035109 (8pp) doi:10.1088/0953-8984/20/03/035109

Electrostatic interaction between two nonuniformly charged colloid particles confined in a long charged cylinder wall

Zengju Lian and Hongru Ma

Department of Physics, Shanghai Jiao Tong University, Shanghai 200240, People's Republic of China

E-mail: hrma@sjtu.edu.cn

Received 8 August 2007, in final form 2 November 2007
Published 17 December 2007
Online at stacks.iop.org/JPhysCM/20/035109

Abstract

The interaction potential of two like-charged colloid spheres with nonuniform surface charge distribution suspended in an electrolyte confined in a long charged cylinder wall is calculated in this paper. Two models of boundary conditions on the cylinder wall are considered. One is the fixed potential model, and the other is the fixed charge density model. The confinement makes a quantitative or even qualitative change to the spheres' interaction compared with the unconfined system. A long-ranged attraction emerges in the confined system, though they are repulsive in the unconfined system under the same other conditions.

1. Introduction

Colloidal solutions are widely applied in industrial processes, in particular in biotechnology, food, pharmaceutical and cosmetics industries because of their many special properties [1–6]. The electrostatic interaction of like-charged colloid particles is one of the most important factors in determining the essential properties of these colloidal solutions, and it was established long ago under the approximation of mean field theory, which predicted a Yukawa type screened repulsion [7, 8]. Yet an anomalous attraction between these particles was suggested by Sogami *et al* [9, 10] in the 1980s and observed in a series of experiments by Grier and other groups [11–18], which ignited a long-lived controversy. Many theoretical investigations of this problem were made and different mechanisms were proposed. However, it seems that different mechanisms can explain different aspects of the experiments and a universally accepted explanation is still lacking [19–25]. It is most noticeable that all the explanations of the anomalous attraction, such as the confinement effect of charged colloids [25], the nonequilibrium hydrodynamic effect [19] and the existence of a metastable ionized state [20], were proposed under one basic assumption. The assumption is that the distribution of charges on the surface of the colloid particles is uniform. However, as found by Tong's group in their experiments [26, 27], in general, charges distribute nonuniformly on colloid spheres such as polystyrene (PS) latex spheres, which are often used in experiments. A very profound attraction between such like-charged colloidal spheres is observed experimentally when the spheres are suspended on the water–air interface [26, 27]. The observed attraction was of the order of several k_BT, much bigger than that observed under the dispersion confinement conditions by other groups [11–16], which was about 0.2 k_BT. The observations of nonuniform distribution of surface charges on the colloid spheres and the profound attraction between these spheres brought about the expectation that the distributions of surface charges on the spheres may play a crucial role in the effective pairwise interaction of charged colloids. Additionally, under the assumption of uniform distribution of surface charges on colloid spheres, Sader *et al* [21] and Neu [22] had rigorously proved that there could not be attractive interaction under the Poisson–Boltzmann approximation. However, it is not clear that this result should still be valid in the case of nonuniform distributions of surface charges on colloid spheres. With these observations, we investigated the interaction between two nonuniformly charged spherical particles immersed in an unbounded electrolyte [28], whose surface charge has the form

$$\sigma(\theta_p, \psi_p) = \sigma_0 \left[1 + b_0 \cos\theta_p\right] \tag{1}$$

where σ_0 denotes the average surface charge density and b_0 is an adjustable parameter characterizing the surface heterogeneity. Uniform distribution of charges on the sphere's surface is a special case of this system with $b_0 = 0$. In this

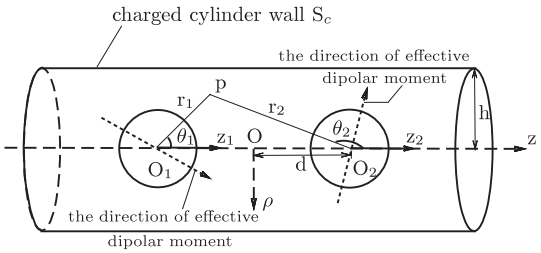

Figure 1. Sketch of the system of two charged spheres in a cylindrical confined polyelectrolyte.

investigation, a long-ranged (compared to the range of van der Waals attraction) electrostatic attraction of two particles emerged when b_0 reached some large value such as $b_0 = 2$ or $b_0 = 3$. Though the positive and negative charges coexist on the sphere's surface when $b_0 > 1$, which is not directly related to the real experiment situations, it is possible that the effective dipolar moment of the colloid particles in real experiments can reach larger values, which may equivalently be represented by a parameter b_0 which is larger than unity [26, 29]. The transition of the interaction between particles from repulsion to attraction with increasing nonuniformity of the distribution of surface charges on the spheres indicated the possibility that the anisotropy of surface charges can be one of the main reasons to produce the anomalous attraction between like-charged colloids.

In general, the distribution of charges on the surface of colloid spheres can be written as $\sigma = \sigma(\theta_p, \psi_p)$, where θ_p and ψ_p are the polar and rotational angles of the spherical coordinates with the z_p axis on the direction of the effective dipolar moment and the origin of these coordinates is on the center of the sphere. This surface charge density can be expanded in terms of spherical harmonics, and can be implemented in the theoretical treatment given in our previous study [28] in a straightforward way for an unbounded system. As an example, in the last part of the paper [28], we also investigated two like-charged colloid particles with a distribution of surface charges that expanded to the second order of the spherical harmonics. The electrostatic interaction of the two like-charged particles for this more general distribution of surface charges was consistent with the one for the simple distribution of equation (1).

In the present study, we extend our calculation to the confined case and study the joint effects of the nonuniform charge distribution and the confinement on the interaction energy between the spheres. In the previous study [28], the electrostatic potential was expressed as a series expansion of spherical harmonics centered in either sphere by using rotation–translation of coordinates. Using the orthogonality of the basis functions, the expansion coefficients can be obtained by solving a set of linear equations resulting from the boundary conditions on the spheres surface. However, the method fails to apply in the present case because of the complexity introduced by the confinement boundary. The difficulty is solved in this study by using the multipole expansion method proposed in the context of the viscous fluid problem by Gluckman and Weinbaum *et al* [30, 31]. Following the idea of the multipole expansion method, we obtain the interaction potentials between two charged spheres with nonuniform distributions of surface charges confined in a long charged cylinder wall.

The paper is organized as follows. In section 2, the basic theory and computation method of the problem is described. A comparison of the interaction potential between the confined system and an unconfined one is given in section 3; other aspects of the interaction are also discussed in this section. Section 4 is the conclusion of the study.

2. The model and method

The model considered is a system of two identical charged colloid spheres with radius a and dielectric constant ϵ_s, confined by a long charged cylinder wall. Three local coordinate systems are used in the representation of the electrostatic potential, which are set up to adhere to the spheres and the cylinder respectively. The origins of these local coordinate systems are at the centers of the spheres and the cylinder respectively and their z-axes are parallel with the cylinder axis. The charge distributions on the colloid spheres, $\sigma(\theta_p, \psi_p)$, can be represented by the local coordinates of the spheres from a rotation of coordinates,

$$\sigma_\alpha(\theta_\alpha, \psi_\alpha) = \hat{D}(\zeta_\alpha, \xi_\alpha, \gamma_\alpha)\sigma(\theta_p, \psi_p) \qquad \alpha = 1, 2. \quad (2)$$

Here, $\hat{D}(\zeta_\alpha, \xi_\alpha, \gamma_\alpha)$ is the rotation operator in which the coordinate system is rotated from the coordinates whose z_p-axis is in the direction of the effective dipolar moment of the sphere to the local coordinate system [32]. ζ_α, ξ_α and γ_α are the three Eulerian angles of the rotation. For example, the surface charge distribution of equation (1) can be written as

$$\begin{aligned}\sigma_\alpha &= \sigma_0(1 + b_0 \cos\theta_p) \\ &= \sigma_0\big[1 + b_0\big(\sin\gamma_\alpha \sin\theta_\alpha \cos(\psi_\alpha - \xi_\alpha) + \cos\gamma_\alpha \cos\theta_\alpha\big)\big] \\ &\alpha = 1, 2. \end{aligned} \quad (3)$$

Besides the local coordinates, we also set up a global coordinate system, which coincides with the local cylindrical coordinate system in this calculation. The local and global coordinates are illustrated in figure 1.

For the sake of computational convenience, all the quantities are represented in the nondimensional form. The unit of length is the sphere's radius, a, and the electrostatic potential ϕ is expressed in dimensionless form as $\Phi = e\beta\phi$. Here $\beta = 1/k_B T$ and k_B, T, e and ϵ_e are the Boltzmann constant, temperature, elementary charge and dielectric constant of the electrolyte respectively.

Under the Poisson–Boltzmann approximation, the dimensionless electrostatic potential in the electrolyte, $\Phi_e = e\beta\phi_e$, for a symmetric 1:1 electrolyte system satisfies

$$\nabla^2\Phi_e(\mathbf{r}) = \frac{2Zc_0\lambda_B}{a}\sinh\left(Z\Phi_e(\mathbf{r})\right). \quad (4)$$

Here $\lambda_B = e^2\beta/\epsilon_e$ is the Bjerrum length, Z is the absolute valence of the ions in the polyelectrolyte and c_0 is the dimensionless concentration (in units of $1/a^3$) of ions at the reference point where $\Phi_e(\mathbf{r}) = 0$. Since we are interested in the effects of the nonuniform charge distribution and

confinement on the colloid particles, we simplify our study by considering the weak potential limit, in which the Poisson–Boltzmann equation is linearized,

$$\nabla^2\Phi_e - b^2\Phi_e = 0. \tag{5}$$

Here $b = \kappa a$ is the dimensionless Debye parameter, κ denotes the Debye parameter and κ^{-1} is a measure of the screening length of the electrostatic interaction, given by

$$\kappa = \sqrt{\frac{2Z^2c_0\lambda_B}{a^3}}. \tag{6}$$

The dimensionless potentials inside the two spheres, $\Phi_s^{(\alpha)} = e\beta\phi_s^{(\alpha)}$, satisfy the Laplace equation

$$\nabla^2\Phi_s^{(\alpha)} = 0, \qquad \alpha = 1, 2. \tag{7}$$

Following the idea of the multipole expansion method, the potential in the electrolyte can be written as a sum of three contributions from three objects, the charged cylinder wall and the two charged spheres. Each part is a linear superposition of the complete solutions of equation (5) which satisfy the boundary conditions at infinity, written in accordance with the respective local coordinates whose origins are placed at the geometrical center of each object.

$$\Phi_e = \sum_t \int F(w,t) I_{|t|}(\sqrt{w^2+b^2}\rho)\mathrm{e}^{\mathrm{i}(wz+t\psi)}\mathrm{d}w + \sum_{\alpha=1,2}\sum_{lm} A_{lm}^{(\alpha)} k_l(br_\alpha) Y_{lm}(\cos\theta_\alpha, \psi_\alpha). \tag{8}$$

The first part of equation (8) denotes the potential due to the charged cylinder wall and the second part is the potential due to the two charged spherical particles. Here, $I_{|t|}(\sqrt{w^2+b^2}\rho)$ is defined as the $|t|$th order modified Bessel function of the first kind, $k_l(br_\alpha)$ is the modified spherical Bessel function of the second kind, $Y_{lm}(\cos\theta_\alpha, \psi_\alpha)$ denotes the spherical harmonics, $\mathrm{i} = \sqrt{-1}$ is the unit imaginary number and l, m and t are integers with $|t|$ and l ranging from 0 to ∞ and $|m| \leqslant l$. Similarly, the potentials inside the two spheres can be expressed by superpositions of basis functions with respect to their local coordinates.

$$\Phi_s^{(\alpha)} = \sum_{lm} B_{lm}^{(\alpha)} r_\alpha^l Y_{lm}(\cos\theta_\alpha, \psi_\alpha), \qquad \alpha = 1, 2. \tag{9}$$

This kind of expansion was first studied in the context of viscous fluid by Weinbaum *et al* as early as 1971 and each term in the expansion subsequently named as a multipole. Similarly, in our case each term of the series in equations (8) and (9) can be viewed as the potential from the multipole and the whole series called the multipole series. The strength of every multipole is given by the coefficients $A_{l,m}^{(\alpha)}$, $B_{l,m}^{(\alpha)}$ and $F(w,t)$. These coefficients are determined by the boundary conditions on the surfaces of the spheres and cylinder wall.

On the surfaces of the spheres the boundary conditions are as follows:

$$\Phi_s^{(\alpha)}(\mathbf{r}_\alpha) = \Phi_e(\mathbf{r}_\alpha), \qquad \mathbf{r}_\alpha \in S_\alpha \tag{10}$$

$$\left(\tau_s\nabla\Phi_s^{(\alpha)}(\mathbf{r}_\alpha) - \nabla\Phi_e(\mathbf{r}_\alpha)\right)\cdot\mathbf{n}_\alpha = \Sigma_\alpha \qquad \mathbf{r}_\alpha \in S_\alpha \tag{11}$$

where S_α represents the surface of particle α, and $\mathbf{n}_\alpha$ is the outer normal unit vector of surface S_α. Σ_α is a dimensionless surface charge density given by $\Sigma_\alpha = \sigma_\alpha ae\beta/\epsilon_e$. $\tau_s = \epsilon_s/\epsilon_e$ denotes the ratio of dielectric constant between the particle and the solvent. On the surface of the cylinder wall, the boundary conditions are related to the structure and the character of the cylinder wall. In real experiments [11–16], glass is usually selected as the charged wall to confine the colloid solution. As a result, the confined boundary is too complex to be treated precisely. To simplify the calculation, we consider here two extreme situations: (a) constant surface potential model on the surface of the cylinder wall; (b) constant surface charge density model on the surface of the cylinder wall. We now give the equations that are needed to solve for the unknown coefficients $A_{l,m}^{(\alpha)}$, $B_{l,m}^{(\alpha)}$ and $F(w,t)$ which appear in the electrostatic potential in the equations (8) and (9) for these two cases of model boundaries.

2.1. The case of constant surface potential on the surface of the cylinder wall

In this model, since the potential on the surface of the cylinder wall is uniform and remains fixed, we can set it to be zero. The boundary condition on the cylinder wall then can be written as

$$\Phi_e(\mathbf{r}) = 0, \qquad \mathbf{r} \in S_c, \tag{12}$$

where S_c denotes the surface of the cylinder wall. Substituting condition (12) into equation (8) yields

$$\sum_t \int F(w,t) I_{|t|}(\sqrt{w^2+b^2}h)\mathrm{e}^{\mathrm{i}(wz+t\psi)}\mathrm{d}w = -\sum_{\alpha=1,2}\sum_{l,m} A_{l,m}^{(\alpha)} k_l(br_\alpha) Y_{l,m}(\cos\theta_\alpha, \psi_\alpha) \qquad \mathbf{r}_\alpha \in S_c, \tag{13}$$

where h is the distance between the spheres and the cylinder wall and $r_1 = \sqrt{h^2+(z+d)^2}$, $r_2 = \sqrt{h^2+(z-d)^2}$, $\cos\theta_1 = (z+d)/\sqrt{h^2+(z+d)^2}$ and $\cos\theta_2 = (z-d)/\sqrt{h^2+(z-d)^2}$. Equation (13) should be satisfied for any points on the inner surface of the cylinder wall, which relates the coefficient $F(w,t)$ to the coefficients $A_{l,m}^{(\alpha)}$. It is obvious that the right-hand side of equation (13) is the two-dimensional Fourier transform of $F(w,t)I_{|t|}(\sqrt{w^2+b^2}h)$. Thus, the coefficient $F(w,t)$ can be expressed directly by coefficients $\{A_{l,m}^{(\alpha)}\}$ through the inverse Fourier transformation:

$$F(w,t) = -\frac{1}{4\pi^2 I_{|t|}(\sqrt{w^2+b^2}h)} \times \int\int \sum_{\alpha=1,2}\sum_{l,m} A_{l,m}^{(\alpha)} k_l(br_\alpha) Y_{l,m}(\cos\theta_\alpha, \psi_\alpha) \times \mathrm{e}^{-\mathrm{i}(wz+t\psi)}\mathrm{d}z\,\mathrm{d}\psi = G(w,t,\{A_{l,m}^{(1)}\},\{A_{l,m}^{(2)}\}) \qquad \mathbf{r}_\alpha \in S_c. \tag{14}$$

Substituting equations (8), (9) and (14) into the spheres' boundary conditions (10) and (11), we obtain

$$\sum_{l,m}\Bigg[B_{l,m}^{(\alpha)}Y_{l,m}(\cos\theta_\alpha,\psi_\alpha)-\sum_{\alpha=1,2}A_{l,m}^{(\alpha)}k_l(b)Y_{l,m}\times(\cos\theta_\alpha,\psi_\alpha)\Bigg]-\sum_t\int G(w,t,\{A_{l,m}^{(1)}\},\{A_{l,m}^{(2)}\})\times I_{|t|}\left(\sqrt{w^2+b^2}\rho\right)\mathrm{e}^{\mathrm{i}(wz+t\psi)}\mathrm{d}w=0,\quad \mathbf{r}_\alpha\in S_\alpha \tag{15}$$

$$\sum_{l,m}\Bigg[\tau_s B_{l,m}^{(\alpha)}lY_{l,m}(\cos\theta_\alpha,\psi_\alpha)-\sum_{\alpha=1,2}A_{l,m}^{(\alpha)}\frac{\partial k_l(br_\alpha)}{\partial r_\alpha}\Bigg|_{r_\alpha=1}Y_{l,m}(\cos\theta_\alpha,\psi_\alpha)\Bigg]-\sum_t\int G(w,t,\{A_{l,m}^{(1)}\},\{A_{l,m}^{(2)}\})\times\frac{\partial I_{|t|}(\sqrt{w^2+b^2}\rho)\mathrm{e}^{\mathrm{i}(wz+t\psi)}}{\partial r_\alpha}\Bigg|_{r_\alpha=1}\mathrm{d}w-\Sigma_s=0,\quad \mathbf{r}_\alpha\in S_\alpha \tag{16}$$

where

$$\rho=r_\alpha\sin\theta_\alpha,$$

$$z=r_1\cos\theta_1-d=r_2\cos\theta_2+d,$$

$$r_1=\sqrt{r_2^2+4d^2+4dr_2\cos\theta_2},$$

$$r_2=\sqrt{r_1^2+4d^2-4dr_1\cos\theta_1},$$

$$\cos\theta_1=(r_2\cos\theta_2+2d)\Big/\sqrt{r_2^2+4d^2+4dr_2\cos\theta_2}$$

and

$$\cos\theta_2=(r_1\cos\theta_1-2d)\Big/\sqrt{r_1^2+4d^2-4dr_1\cos\theta_1}$$

with the reduced center–center distance of spheres $2d$. The key point of the multipole expansion method is that the coefficients $A_{l,m}^{(\alpha)}$, $B_{l,m}^{(\alpha)}$ are determined by substituting a discrete set of points on the boundaries S_α into equations (15) and (16). In the complete expansion, there are an infinite number of coefficients to be determined, thus the expansion has to be truncated at some value of $l_{\max}=N$ in numerical calculations. In this case we are left with $4(N+1)^2$ coefficients to be determined; we then choose $(N+1)^2$ points on each sphere's surface and substitute the coordinates of the chosen points into equations (15) and (16) to form a set of $4(N+1)^2$ equations. It should be noted that all the coefficients are complex numbers. For a special axial symmetry distribution of surface charge on the sphere such as the distribution of equation (1), when the directions of effective dipolar moments of the two spheres are both on the cylinder axis, z, the system is axially symmetric around z. Thus the potentials are independent of the angle ψ and ψ_α, i.e. $m=t=0$. As a result, the number of coefficients is reduced from $4(N+1)^2$ to $4N$. Then N points on the sphere's generatrix are enough to solve these coefficients. It is noticeable that, here, due to the axial symmetry of the problem, each point on the sphere's generatrix denotes one circle on the sphere's surface. The set of equations is solved numerically to obtain the required coefficients. Since the truncated equations are approximations of the complete equations, different choices of points on the boundaries may give different solutions of the expansion coefficients. It is also possible that some sets of points result in equations where the solution is not uniquely determined. This kind of question is studied in the context of viscous flow problems and some useful guidelines and convergence analysis are available [30, 31]. In our calculation we choose the points by guidance from viscous flow studies and check the convergence by successive increase of the order of truncation and by comparing the results from different sets of points used in calculations. In real calculations, we find that N decreases with increasing colloid–colloid distance and $N=24$ is enough to obtain an accurate potential at the short distance of about $2d=2.2$ for an axial symmetry system. The equations are solved by an iterative method. First, for initial guess of the coefficients $\{A_{l,m}^{(\alpha)}\}$ and $\{B_{l,m}^{(\alpha)}\}$, $F(w,t)$ is obtained from equation (14) through fast Fourier transformation, then the results inserted into equations (15) and (16) to form a set of linear equations for $\{A_{l,m}^{\alpha}\}$ and $\{B_{l,m}^{\alpha}\}$, which can easily be solved, and the results are used as input for the next iteration. This simple iteration scheme converges to the desired accuracy after six iterations for the axial symmetry system; here, the accuracy was specified as a relative error of the coefficients between iterations less than 10^{-7}. We denote the surface charge density on the cylinder surface as σ_c, then the dimensionless charge density $\Sigma_c=\sigma_c ae\beta/\epsilon_0$ is given by

$$\Sigma_c=\nabla\Phi_e(\mathbf{r})\cdot\mathbf{n}_c,\qquad \mathbf{r}\in S_c. \tag{17}$$

The electroneutral condition of the system is automatically satisfied in this case and is checked in the numerical calculation.

2.2. The case of constant surface charge density on the surface of the cylinder wall

For the model of constant surface charge density on the cylinder wall, there are similar conditions with equations (10) and (11) on the surface of the cylinder wall,

$$\Phi_c(\mathbf{r})=\Phi_e(\mathbf{r}),\qquad \mathbf{r}\in S_c \tag{18}$$

$$(\nabla\Phi_e(\mathbf{r})-\tau_c\nabla\Phi_c(\mathbf{r}))\cdot\mathbf{n}_c=\Sigma_c\qquad \mathbf{r}\in S_c. \tag{19}$$

Here $\Phi_c=e\beta\phi_c$ denotes the dimensionless potential inside the cylinder wall; $\tau_c=\epsilon_c/\epsilon_e$ is the dielectric constant ratio between the cylinder wall and the fluid. Note that the potential Φ_c can only be determined when the structure and boundary conditions of the cylinder wall are specified. For simplicity, we assume that there are no free ions inside the wall and there is no outer boundary of the wall, which implies that the potential Φ_c satisfies the Laplace equation and decays to zero at infinity. Thus the potential Φ_c can be expressed as

$$\Phi_c=\sum_t\int H(w,t)K_{|t|}(|w|\rho)\mathrm{e}^{\mathrm{i}(wz+t\psi)}\mathrm{d}w. \tag{20}$$

Here, $K_{|t|}(|w|\rho)$ is the modified Bessel function of the second kind and $H(w,t)$ is the expansion coefficient to be determined

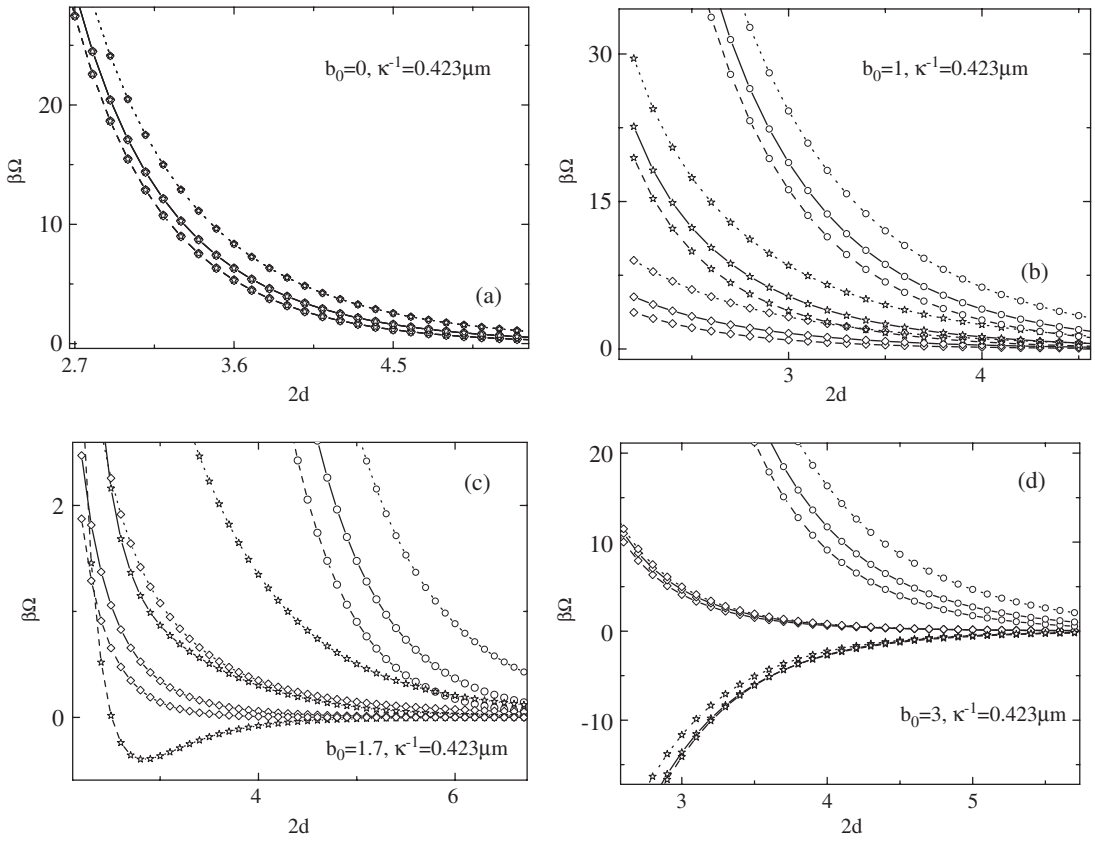

Figure 2. The interaction energy of two spheres as a function of the reduced colloid–colloid distance with different boundary conditions on the cylinder wall: fixed potential, − − −; fixed charge density, · · ·. Distribution of surface charge on the spheres: (a) $b_0 = 0$ (uniform distribution); (b) $b_0 = 1$; (c) $b_0 = 1.7$; (d) $b_0 = 3$. In each subfigure, the head–head case is denoted by ○, the tail–tail case is denoted by ◇ and the parallel case is denoted by ⋆. For comparison, the bulk (unconfined) case is plotted as solid lines in each part of the figure.

by the boundary conditions (10), (11), (18) and (19). The electroneutral condition of the system is satisfied automatically when the conditions (10), (11), (18) and (19) are satisfied.

Substituting equation (20) and (8) into the two boundary conditions (18) and (19) yields

$$\sum_t \int \left[H(w,t)K_{|t|}(|w|h) - F(w,t)I_{|t|}\left(\sqrt{w^2+b^2}h\right)\right] \times \mathrm{e}^{\mathrm{i}(wz+t\psi)}\mathrm{d}w = \sum_{\alpha=1,2}\sum_{l,m} A_{l,m}^{(\alpha)} k_l(br_\alpha) Y_{l,m}(\cos\theta_\alpha, \psi_\alpha), \quad \mathbf{r}_\alpha \in S_c \tag{21}$$

$$\sum_t \int \left[\tau_c H(w,t)\frac{\partial K_{|t|}(|w|\rho)}{\partial\rho} - F(w,t)\frac{\partial I_{|t|}(\sqrt{w^2+b^2}\rho)}{\partial\rho}\right]_{\rho=h} \mathrm{e}^{\mathrm{i}(wz+t\psi)}\mathrm{d}w = \sum_{\alpha=1,2}\sum_{l,m} A_{l,m}^{(\alpha)} \left.\frac{\partial[k_l(br_\alpha)Y_{l,m}(\cos\theta_\alpha,\psi_\alpha)]}{\partial\rho}\right|_{\rho=h} - \Sigma_c, \quad \mathbf{r}_\alpha \in S_c. \tag{22}$$

Here,

$$r_1 = \sqrt{\rho^2 + (z+d)^2},$$

$$r_2 = \sqrt{\rho^2 + (z-d)^2},$$

$$\cos\theta_1 = (z+d)/\sqrt{\rho^2+(z+d)^2}$$

and

$$\cos\theta_2 = (z-d)/\sqrt{\rho^2+(z-d)^2}.$$

Similarly, the right-hand sides of equations (21) and (22) are Fourier transforms of the left-hand sides of (21) and (22), respectively. After inverse Fourier transforms, $F(w,t)$ and $H(w,t)$ can be expressed in terms of $\{A_{l,m}^{(\alpha)}\}$, $\alpha = 1, 2$

$$F(w,t) = G_1(w,t,\{A_{l,m}^{(1)}\},\ \{A_{l,m}^{(2)}\}) \tag{23}$$

$$H(w,t) = G_2(w,t,\{A_{l,m}^{(1)}\},\ \{A_{l,m}^{(2)}\}). \tag{24}$$

Substituting equation (23) into the potential in the electrolyte Φ_e and using the sphere boundary conditions (10) and (11), we obtain similar equations to (15) and (16) when $G(w,t,\{A_{l,m}^{(1)}\},\{A_{l,m}^{(2)}\})$ is replaced with $G_1(w,t,\{A_{l,m}^{(1)}\},\{A_{l,m}^{(2)}\})$. The equations can be truncated and solved numerically with the same method as used in the case of the constant potential model.

3. The interaction potential between two spheres

Under the linear approximation, once the potential is obtained, the interaction energy between the two spheres can be written

as a sum of surface integrals over each sphere and cylinder wall [28]:

$$\beta\Omega = \frac{a}{2\lambda_B}\left[\sum_{\alpha=1,2}\int \mathrm{d}S_\alpha \Phi_e \Sigma_\alpha + \int \mathrm{d}S_c \Phi_e \Sigma_c\right] - \beta W_0, \tag{25}$$

where βW_0 is a constant energy due to the Coulomb potential of the system when the center–center distance of the two spheres tends to infinity. In fact, we never mention the concrete form of the surface charge distribution of spheres throughout section 2 and equation (25). That means that the theories in section 2 and equation (25) are valid for any distribution of charges on the sphere's surface.

The interaction energy in equation (25) is for a given configuration of the two spheres. In real experiments, however, colloid spheres can rotate due to thermal agitations; an instantaneous interaction potential obtained for a specified configuration of the two colloid spheres does not represent the experimentally measured one. In order to get experimentally comparable results, we have to calculate the potentials for all the possible orientations and average the results with a Boltzmann factor, which requires a large number of numerical calculations, and the task is formidable. Additionally, since the distribution of the surface charges on the particles can be expanded in terms of spherical harmonics and we here are only interested in the effect of charge nonuniformity on the effective interaction of two like-charged colloid particles, we can simplify our model and consider a simple distribution of surface charge on the spheres with equation (1) [28]. We also assume the directions of the effective dipolar moments of two spheres are parallel or antiparallel to the axis of the cylinder, z. In this way the problem is reduced to a two-dimensional problem. Though the situation we consider here is a special one, it can already illuminate the problems we are investigating in some way.

Some parameters in our calculations are characterized in table 1. Here we select average surface charge density $\sigma_0 = 25.5\ \mu\mathrm{C\ m^{-2}}$, i.e., the value of total charge $Q = 500$, which is lower than the cases of experiment setups [11–16, 26, 27]. The choice of the small total charge in our calculation is simply because of the linear approximation requirement of weak potential. In fact, when the number of charges on the spheres reaches some high value, it will renormalize [33] and the full nonlinear theory has to be used in the calculation. Figure 2 shows the results of the interaction potential between two like-charged colloid spheres as a function of the reduced colloid–colloid distance of the two spheres, $2d$, with four different nonuniform distributions of surface charges on the spheres, corresponding to the parameters $b_0 = 0$, $b_0 = 1$, $b_0 = 1.7$ and $b_0 = 3$ respectively. In order to specify the configurations of the spheres, we first define the head and tail of a colloid sphere as the two poles with maximum and minimum charge densities respectively; then the three cases we studied are (a) head–head antiparallel, in which the two heads of the two spheres are directed to each other, (b) tail–tail antiparallel, in which the two tails of the two spheres are directed to each other, and (c) parallel, in which both the spheres are in the same direction.

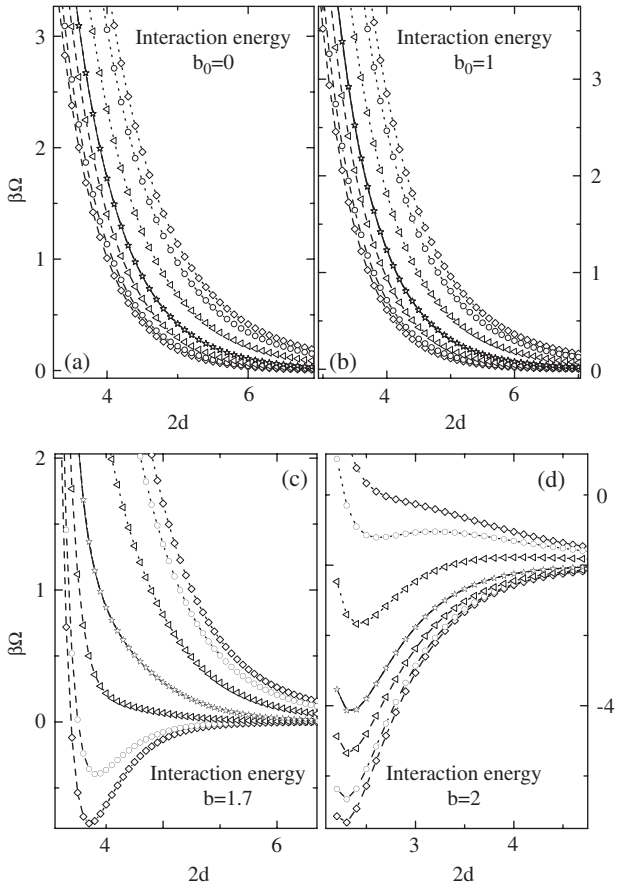

Figure 3. The interaction energy of two spheres as a function of the colloid–colloid distance with different sphere–wall separations h: $h = 2.0$, ◇; $h = 2.13$, ○; $h = 2.5$, ◁; $h = 10.0$, ⋆. The boundary conditions on the cylinder wall are the following: fixed potential, − − −; fixed surface charge density $\sigma_c = 0.2\sigma_0$, · · ·; unconfined system, —. The charge distributions on the spheres are (a) $b_0 = 0$; (b) $b_0 = 1$; (c) $b_0 = 1.7$; (d) $b_0 = 2$. Here the curves for the case of the unconfined system and $h = 10$ for both the fixed potential model and the fixed charge density model superpose each other.

From figure 2, we see that the interaction between two spheres in the head–head case is always repulsive. The tail-tail case is also repulsive, and the repulsion is weaker than both the head–head and parallel cases when b_0 is small, and turns into the second when b_0 is increased close to 1.7. The most interesting case is the parallel case, which is repulsive at small b_0 and turns to attractive when the anisotropy parameter b_0 increases. The transition from the repulsion to attraction is due to the interaction of effective dipoles arising from anisotropy of surface charges on the spheres' surfaces. In general, the interaction energy between two spheres is the result of the competition of the attractive interaction between effective dipoles and repulsion between two effective charges if the contributions of higher multipoles are neglected. For the surface charge distribution of equation (1), the effective dipolar moment is $\frac{4}{3}b_0\pi a^3\sigma_0$, which increases with b_0.

The confinement on the spheres also modifies the interaction energy. In figure 2, we see that the spheres are more repulsive or less attractive at short colloid–colloid distance for the unconfined case than for the case of the model

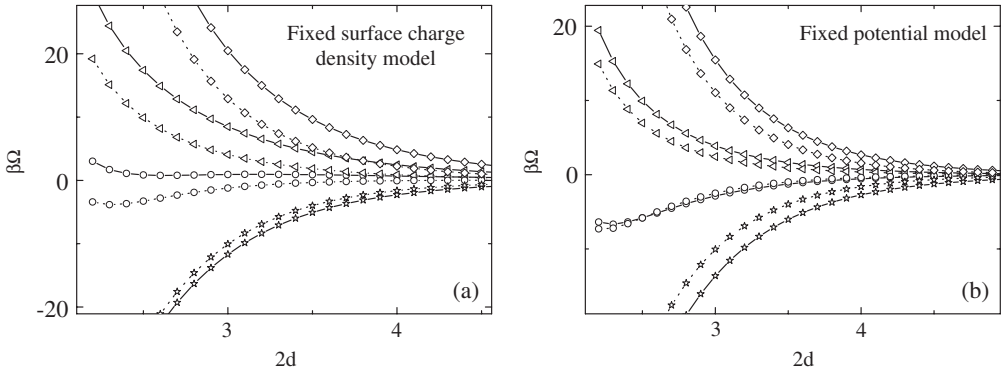

Figure 4. The interaction energy of two spheres as a function of colloid–colloid distance with different values of c_0: $c_0 = 80.0$, corresponding to $\kappa^{-1} = 0.423$ μm, —; $c_0 = 120.0$, corresponding to $\kappa^{-1} = 0.234$ μm, $\cdots$. Distribution of surface charges on the spheres: $b_0 = 0$, $\diamond$; $b_0 = 1$, $\triangleleft$; $b_0 = 2$, $\circ$; $b_0 = 3$, $\star$. Boundary conditions on the cylinder: (a) fixed surface charge density; (b) fixed potential.

Table 1. Some parameters selected in our calculations; here ϵ_0 is the vacuum dielectric constant.

T	τ_s	τ_c	ϵ_e	a	σ_0	σ_c	Z	κ^{-1}	h
300 K	0.0625	0.075	$80\epsilon_0$	0.5 μm	25.5 μC m^{-2}	$0.2\sigma_0$	1	0.423 μm	2.13

of fixed potential on the cylinder wall, while they are less repulsive or more attractive than for the case of the model of fixed surface charge density on the cylinder wall. This phenomenon implies that the electrostatic repulsion is more effectively screened by the electrolyte for the fixed potential model than that for the unconfined system, while the fixed surface charge density model is just the opposite. In the case of $b_0 = 1.7$ for the parallel configuration case seen in figure 2(c), the confinement of the cylinder wall with fixed potential produces an attraction between two spheres, while these spheres are purely repulsive in the unconfined system. This significant change between the unconfined system and confined system for the spheres' interaction indicates that the confinement on the charged colloid particles might also be one of the important reasons to induce the attraction between two like-charged particles.

A comparison of interaction energies for the parallel case with various sphere–wall separations, h, is shown in figure 3. In the case of the fixed potential model, the interaction energy increases when h increases for the four different distributions of surface charges on the spheres, $b_0 = 0$, $b_0 = 1$, $b_0 = 1.7$ and $b_0 = 2$, and with the increasing of h, the interaction tends to the bulk case denoted by solid lines (superposed with the curves of $h = 10$ and barely distinguishable), which gives a consistency check of our calculations. In the case of the constant charge density model, the situation is just the opposite: the interaction energy is decreasing at the short colloid–colloid distance when h increases. Similarly, the interaction tends to the bulk case as h increases. It is most noticeable that the reduction of the sphere–wall separation also qualitatively changes the interaction for both $b_0 = 1.7$ and $b_0 = 2$ in figures 3(c) and (d). Under the confinement of a charged cylinder wall whose potential is fixed, a minimum consistent with a long-ranged attraction emerges for the case of $b_0 = 1.7$ with the reduction of h, while for the case of $b_0 = 2$ the minimum vanishes as h decreases under the confinement of a charged cylinder wall whose surface charges are fixed.

Figure 4 shows the results of interaction energies of two spheres with different relative concentrations of ions c_0 at $\Phi_e = 0$ as a function of the colloid–colloid separation $2d$. The interaction between two spheres tends to zero more quickly as c_0 increases whether for the fixed potential model or the fixed charge density model. This is a trivial result since the Debye screening length is in inverse proportion to $c_0^{1/2}$, as can be seen in equation (6). The interesting result here is that two repulsive spheres become attractive with the enhancement of c_0 for the case of $b_0 = 2$ in the fixed surface charge density model seen in figure 4(a). Additionally, in the case of the fixed charge density model, the density of charges on the cylinder surface, σ_c, is also one of the important parameters directly affecting the interaction energy. Figure 5 represents the effect of different σ_c on the interaction energies for the four different surface charge distributions on the spheres. From this figure, we see that the effective charge repulsion is more effectively screened with decreasing σ_c. Some qualitative changes of the spheres' interaction also occur for $b_0 = 2$ as the σ_c decreases.

4. Conclusion

In summary, we have investigated a system of two nonuniformly like-charged colloid spheres suspended in an electrolyte confined in a long charged cylinder wall. Two kinds of boundary conditions on the surface of cylinder wall are considered in this system: one is the constant potential model and the other is the constant surface charge density model. Compared with the unconfined system, the confinement quantitatively and even qualitatively changes the interaction between two charged spheres under the approximation of linear Poisson–Boltzmann theory. A long-ranged attraction between two like-charged spheres emerges in the confined

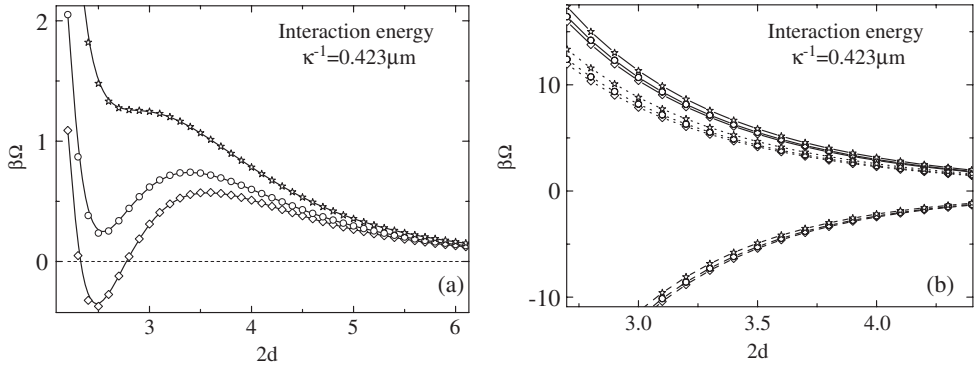

Figure 5. The interaction energy of spheres as a function of the sphere center–center distance for the fixed charge density model with different values of charge densities on the cylinder wall: $\sigma_c = -0.2\sigma_0$, ◇; $\sigma_c = 0$, ○; $\sigma_c = 0.2\sigma_s$, ⋆. Distribution of surface charges on the spheres: (a) $b_0 = 2$; (b) $b_0 = 0$, —; $b_0 = 1$, $\cdots$; $b_0 = 3$, $- - -$.

system, though it is repulsive in the unconfined system of the same other environment parameters as given in table 1. This phenomenon suggests that the confinement of spheres is also one of the important reasons to induce a long-ranged attraction. Under the confinement of a long charged cylinder wall, the sphere–wall separation, the density of surface charges on the cylinder wall and the ion concentration in the electrolyte also significantly affect the spheres' interaction.

Acknowledgments

The work is supported by the National Natural Science Foundation of China under grant Nos 90103035, 10334020 and 10174041.

References

[1] Schwarz K, Huang S W, German J B, Tiersch B, Hartmann J and Frankel E N 2000 *J. Agricult. Food Chem.* **48** 4874
[2] Jauregi P and Varley J 1999 *Trends Biotechnol.* **17** 389
[3] Freeman I P, Padley F B and Sheppard W L 1973 *J. Am. Oil Chem. Soc.* **50** 101
[4] Segawa T, Kamata M, Hara S and Totani Y 1995 *J. Japan. Oil Chem. Soc.* **44** 36
[5] Koga T and Terao J 1995 *J. Agricult. Food Chem.* **43** 1450
[6] Huang S W, Frankel E N, Aeschbach R and German J B 1997 *J. Agricult. Food Chem.* **45** 1991
[7] Derjaguin B V and Landau L 1941 *Acta Physicochim. (URSS)* **14** 633
[8] Verwey E J and Overbeek J T G 1948 *Theory of the Stability of Lyophobic Colloids* (Amsterdam: Elsevier)
[9] Sogami I 1983 *Phys. Lett.* A **96** 199
[10] Sogami I and Ise N 1984 *J. Chem. Phys.* **81** 6320
[11] Crocker J C and Grier D G 1994 *Phys. Rev. Lett.* **73** 352
[12] Crocker J C and Grier D G 1996 *Phys. Rev. Lett.* **77** 1897
[13] Larsen A E and Grier D G 1997 *Nature* **385** 230
[14] Han Y and Grier D G 2003 *Phys. Rev. Lett.* **91** 038302
[15] Behrens S H and Grier D G 2001 *Phys. Rev.* E **64** 050401
[16] Grier D G and Han Y 2004 *J. Phys.: Condens. Matter* **16** S4145
[17] Kepler G M and Fraden S 1994 *Phys. Rev. Lett.* **73** 356
[18] Acuña-Campa H, Carbajal-Tinoco M D, Arauz-Lara J L and Medina-Noyola M 1998 *Phys. Rev. Lett.* **80** 5802
[19] Squires T M and Brenner M P 2000 *Phys. Rev. Lett.* **85** 4976
[20] Messina R, Holm C and Kremer K 2000 *Phys. Rev. Lett.* **85** 872
[21] Sader J E and Chan D Y C 1999 *J. Colloid Interface Sci.* **213** 268
[22] Neu J C 1999 *Phys. Rev. Lett.* **82** 1072
[23] Bowen W R and Sharif A O 1998 *Nature* **393** 663
[24] Danos M and Maximon L C 1965 *J. Math. Phys.* **6** 766
[25] Löwen H, Madden P A and Hansen J P 1992 *Phys. Rev. Lett.* **68** 1081
Löwen H, Hansen J P and Madden P A 1993 *J. Chem. Phys.* **98** 3275
[26] Chen W, Tan S, Ng T K, Ford W T and Tong P 2005 *Phys. Rev. Lett.* **95** 218301
[27] Chen W, Tan S, Huang Z, Ng T K, Ford W T and Tong P 2006 *Phys. Rev.* E **74** 021406
[28] Lian Z J and Ma H R 2007 *J. Chem. Phys.* **127** 104507
[29] Hoffmann N, Christos N L and Hansen J P 2004 *Mol. Phys.* **102** 857
[30] Gluckman M J, Pfeffer R and Weinbaum S 1971 *J. Fluid Mech.* **50** 705
[31] Weinbaum S, Ganatos P and Yan Z Y 1990 *Annu. Rev. Fluid Mech.* **22** 275
[32] Ka X L 2001 *Advanced Quantum Mechanics* (China: Higher Education Press) p 301
[33] Alexander S, Chaikin P M, Grant P, Morales G J, Pincus P and Hone D 1984 *J. Chem. Phys.* **80** 5776